Eighth South African Conference on Computational and Applied Mechanics
SACAM2012
Johannesburg, South Africa, 3−5 September 2012

Finite element modeling of corneal strip extensometry

N. Botha*†, S. Kok* and H.M. Inglis†
*Advanced Mathematical Modelling
CSIR Modelling and Digital Sciences, PO Box 395, Pretoria, South Africa, 0001
Email: nbotha1@csir.co.za
†Department of Mechanical and Aeronautical Engineering
University of Pretoria, Pretoria, South Africa, 0001

***Abstract*—Corneal biomechanical properties are an important element in the study of corneal biomechanics. There are currently two techniques to obtain these properties; an inflation test and the strip extensiometry test. As the inflation test has been numerically modelled in several studies, this study focusses on accurately modelling the strip extensiometry test. Two methods were considered to simulate the experimental conditions namely, a single phase and a two phase method.**

A finite element model of the corneal strip specimen was developed using an elastic fibre reinforced constitutive model to describe the corneal microstructure. The experimental conditions were simulated by defining prescribed displacements to simulate the required phases for each method.

The results indicated that by using the two phase method, which is a more accurate description of the experimental setup, that no additional post processing is required to obtain a reaction force response which correlates with experimental data.

***Keywords*—cornea; strip extensometry; finite element analysis**

INTRODUCTION

Corneal biomechanical properties are a crucial element to not only understanding the corneal behaviour and responses, but also to accurately quantify other properties such as intraocular pressure (IOP) measurement. It is also known that intraocular pressure (IOP), which is an important risk identifier for glaucoma, is sensitive to corneal material properties [1] [2]. Corneal properties are determined by means of two popular techniques; the inflation test and strip extensometry test.

In the inflation test, a whole corneal specimen is clamped onto a pressure chamber and then inflated beyond its physical limitations. This test, however, only accounts for the isotropic behaviour of the cornea, which is considered adequate when focussing on large scale effects. But as soon as the problem under consideration involves small scale effects it is required to also account for the anisotropic behaviour of the cornea due to the embedded fibers. The inflation test has been numerically simulated in several studies [3] [4] [5] [6] to obtain corneal material properties.

To obtain material properties which take the microscopic structure of the cornea into account a strip extensometry test is performed. For the strip extensometry test, a strip of the corneal tissue, with a constant width, is dissected from a corneal specimen (Fig. 1a) in the vertical and diagonal directions as illustrated in Fig. 2. The corneal specimen is then

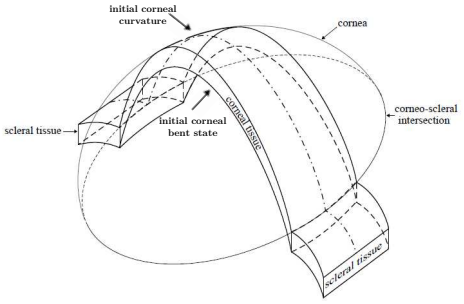

(a) Corneal strip specimen

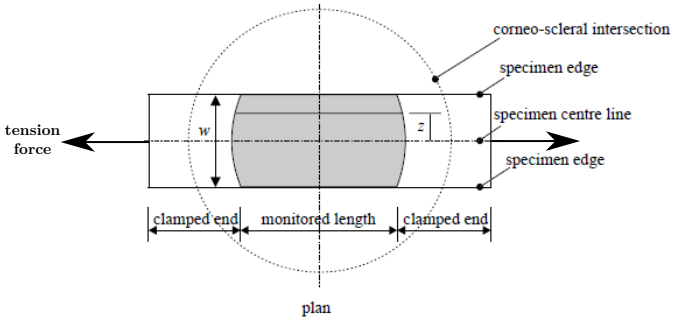

(b) Experimental setup for strip extensometry test

Fig. 1: Illustration of the (a) corneal specimen dissected from a cornea indicating the initial corneal curvature and bent state and (b) the experimental setup showing that part of the cornea is also clamped along with the sclera. (Taken from Elsheikh and Anderson [7])

clamped into position on a slow rate tension machine, where it is then elongated by applying a tension force (Fig. 1b). This activates the microstructural embedded fibres, which contribute to the anisotropic behaviour of the cornea. However this test is less popular than the inflation test as it is believed to be less reliable [7].

Extensive experimental studies have been conducted over the years to quantify corneal material properties using the strip extensometry test [8] [9] [10] [11] [12] [13]. However, from a modelling point of view few studies have used the strip extensometry test to quantify corneal material properties [14] [15]. Coincidentaly both these studies used the inflation test

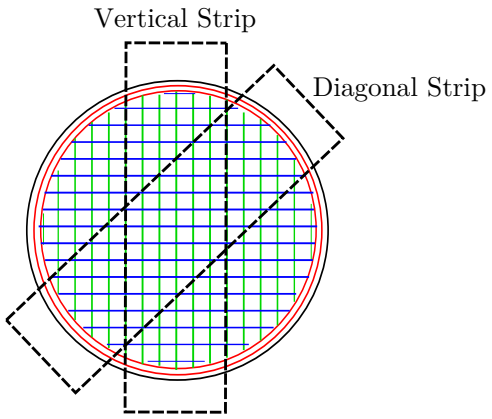

Fig. 2: Preferred fibre directions of the collagen fibrils, (i) circumferential fibres along the limbus (red), (ii) orthogonal fibres in the central cornea (green and blue); and the vertical and diagonal strips dissected from a corneal specimen (dashed lines)

together with the strip extensometry test to more accurately quantify the anisotropic behaviour of the cornea.

Pandolfi and Manganiello [14] reproduced a strip extensometry test with an applied tension in the direction of the first set of fibers (vertical). Even though material properties were obtained using this model that captured the anisotropic behaviour for a range of strip experimental data, not much detail is given as to how the strip test was simulated. There were also discrepancies between the material properties obtained from the strip and inflation simulations.

Studer et al. [15] focussed on solving this problem of Pandolfi and Manganiello [14] by developing a material model, which not only incorporates the collagen fiber microstructure, but also fits both inflation and strip experimental data. They succeeded in developing such a model which fit both sets of data, however their approach for modelling the strip extensometry test does not correspond to the actual experimental setup. They modelled the corneal strip by only clamping a portion of the sclera and simply applying a tension force. With this approach it is difficult to distinguish the flattening of the cornea from the elongation when analysing the results. It appears that Studer et al. [15] accounted for this by amending the material model with a crimping factor.

The objective of this study is to develop a finite element model of the corneal strip extensometry test that more accurately simulates the actual experimental setup. A two phase simulation process is proposed where the clamping and elongation of the corneal strip during an experimental setup is simulated separately. A single phase simulation process is also considered, where the corneal strip is flattened and elongated in a single motion. This study will also only focus on modeling of the vertical strip as the current material model is not able to accurately capture the expected behaviour of the cornea in the case of a diagonal strip.

Materials and Methods

A. Constitutive model

Microscopically, the cornea is primarily composed of collagen fibrils which are orientated orthogonally to other fibrils. These preferred collagen orientations [16] are illustrated in Fig. 2. The directionality of the fibrils changes as it approaches the limbus from orthogonal to circumferential. The cornea is also considered to be viscoelastic and incompressible as the stroma, consisting of 80% water, comprises 90% of its thickness.

The constitutive model used in this study is therefore an anisotropic model with an isotropic neo-Hookean base and exponential term to describe the response of the embedded corneal fibres [17] [18]. The strain-energy density function is described mathematically [17] [18] as:

$$U = C_{10}(\bar{I}_1 - 3) + \frac{1}{D_1}(\bar{J} - 1)^2 + \sum_{i=4,6}^{n} \frac{k_{1i}}{2k_{2i}}[e^{(\bar{I}_i - 1)^2} - 1], \quad (1)$$

where C_{10} and k_{1i} are stress-like material parameters, D_1 is an incompressibility constant, k_{2i} is a dimensionless parameter and $\bar{I}_1$ and $\bar{I}_i$ are invariants. The first and third terms in (1) describe the isotropic response of the non-collagenous matrix material and the anisotropic response due to the embedded collagen fibers, respectively.

To simplify the analysis, only the orthogonal fibres in the central cornea are modeled. It is also assumed that the fibre stiffness is the same for both sets of fibres [14]. The number of material coefficients is therefore reduced from six to four, as $k_{14} = k_{16} = k_1$ and $k_{24} = k_{26} = k_2$ (cf. (1)).

This model was chosen as it has been demonstrated to adequately describe the corneal microstructure [14] and is already available in Calculix [17], an open-source finite element solver. However, this model is not able to accurately capture the expected anisotropic response in the case of the diagonal strip. Instead a linear response is obtained, which indicates that the embedded fibres are not activated during tension. This is a limitation of the constitutive model as there will be a small distribution of fibres present in the diagonal direction such that it contributes to the anisotropic response [15] [14]. Due to this limitation in the chosen constitutive model only the vertical strip is modelled. The diagonal strip will be modelled in future studies once the current constitutive model is improved upon.

B. Cornea strip finite element model

To generate the finite element model of the corneal specimen (c.f. Fig. 1a) the geometric data as described by Elsheikh et al. [12] was used. The cornea strip has a width of 3 mm, a central corneal thickness of 0.572 mm, with an initial arc length of 10 mm along the neutral axis of the cornea. The anterior and posterior radius of curvature is taken to be 7.78 mm and 6.40 mm respectively [2]. The cornea geometry was then generated, in its initial bent state with the initial corneal curvature, by describing the aspherical shape as a rotationally symmetric conicoid [19]:

$$(x - x_o)^2 + (y - y_o)^2 + (1 + Q)(z - z_o)^2 - 2R(z - z_o)^2 = 0, \quad (2)$$

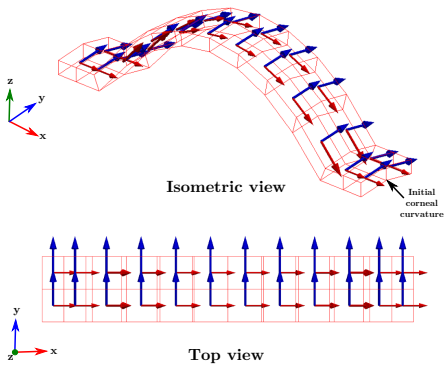

Fig. 3: Finite element model of the vertical corneal strip, including the orthogonal fibres.

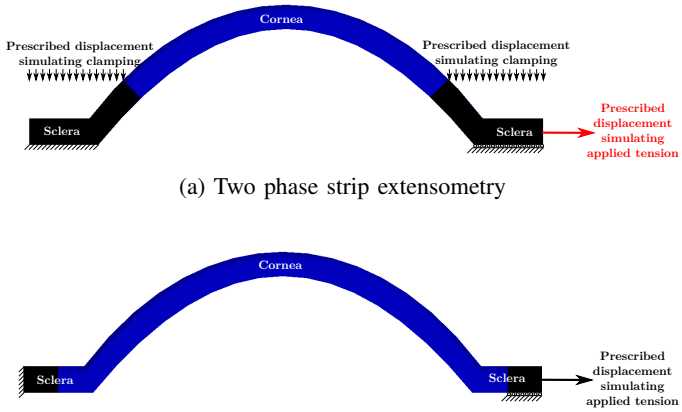

(a) Two phase strip extensometry

(b) Single phase strip extensometry

Fig. 4: Illustration of the single and two phase methods used to simulate the strip extensometry test. The black regions on the cornea indicate the clamped areas. (a) For the two phase method: the first phase is indicated in black and the second phase in red. (b) For the single phase method the phase is indicated in only black.

where R is the radius of curvature at the corneal apex, Q is the surface asphericity parameter (-0.18 anteriorly and -0.60 posteriorly [2]), x is the distance along the equator axis, y is the distance along the sagittal axis and z, the optical axis, is the axis of rotation.

To accurately simulate the experimental corneal strip, an additional 2 mm of scleral tissue is added to each end of the modeled strip. The fibre directions for the vertical strip, shown in Fig. 2, are also included in the constitutive model to complete the numerical model. The finite element strip model, in its initial bent state, with the vertical fibre directions is shown in Fig. 3.

C. Strip extensometry simulation

The strip extensometry experimental setup is simulated with two methods. The first method is known as the two phase method, where the clamping of the corneal strip is simulated as the first phase and the elongation of the strip as the second phase. The second method is known as the single phase method in which a tension is applied and the corneal strip is flattened and elongated in a single motion. This section aims to explain the methods used to set up each of the numerical simulations found in published literature.

TWO PHASE METHOD: The experimental clamping action for phase one is simulated by defining a prescribed displacement on the anterior surface of the corneal strip (including a small section of the cornea along with the sclera). A fixed boundary condition is also applied to the posterior surface of the sclera on the left hand side, while the portion of the sclera on the right hand side is fixed to only allow for translation in the direction of the applied tension. After the corneal specimen is flattened in phase one, the sample is elongated in tension by applying a set of prescribed displacements on the side face of the sclera on the right hand side. These boundary conditions are shown in Fig. 4a, where phase one is illustrated in black and phase two in red.

SINGLE PHASE METHOD: The single phase method assumes that only a small section of the sclera is clamped during the experimental setup. This is simulated by applying a fixed boundary condition to the left face of the sclera on the left hand side, not allowing for any translation or rotation. The tension force is then simulated with a prescribed displacement, and translation of the scleral portion on the right hand side is only allowed in the direction of this applied displacement. This model neglects the actual clamping of the specimen in the experimental setup. As the specimen is pulled in tension from the initial bent state, it is first flattened (creating the illusion of clamping) before continueing to elongate it in a single motion. The boundary conditions for the single phase method are shown in Fig. 4b.

D. Optimization of material coefficients

The material coefficients required to describe the corneal material were identified by solving an unconstrained optimization problem. The Nelder-Mead simplex method as implemented in the SciPy module [20] was used to minimize the root mean square error for the vertical strip test. The objective function was defined as:

$$\min F(\mathbf{X}) = \sqrt{\frac{\sum_{i=1}^{n}(y_{2i} - y_{1i})^2}{n}}, \tag{3}$$

where y_{2i} is the experimental data set and y_{1i} is the numerical data set. In (3), $\mathbf{X}$ is a vector containing the three material coefficients, C_{10}, k_1 and k_2 (cf. (1)). Note that for the process of optimizing the material coefficients only the two phase method is used.

Results and Discussion

E. Calibration of material coefficients

The optimum material coefficients, obtained from the optimization process, are listed in Table I for two different age groups [12]. Note that the incompressibility parameter, D_1,

is fixed at 0.004, which ensures the incompressibility of the material model. The corresponding extensometry test results obtained for the vertical strip are shown in Fig. 5 for each age group.

It is widely known that corneal material properties are dependent on age and tends to become stiffer with an increase in age [13], which is clear when comparing the results in Table I and Fig. 5 for both age groups.

TABLE I: List of optimum material coefficients obtained from the optimization process for two different age groups. (C_{10} and k_1 are in MPa; and D_1 and k_2 are dimensionless)

	$\mathbf{C}_{10}$	$\mathbf{D}_1$	$\mathbf{k}_1$	$\mathbf{k}_2$	**RMSE**
Age Group 1 (69-70 years)	0.8651	0.004	1.1083	20.6241	3.9519%
Age Group 2 (96-97 years)	0.9207	0.004	0.2470	52.2845	15.7845%

It is interesting to note that the experimental data in Fig. 5 appears to have strong linear characteristics for the first few millimeters, suggesting that the fibers are immediately active during elongation of the specimen. It is also noted that in Fig. 5b the constitutive model is unable to accurately capture the linear behaviour of the first 0.75 mm. It is assumed that this portion of the experimental data will only be accurately captured once a distribution of fibers are introduced into the constitutive model, instead of only having two distinct families of fibers.

F. Comparison of the simulation methods

In this section the two methods of simulating the experimental setup as described by Elsheikh et al. [12] is compared. The results for both simulations are shown in Fig. 6, where it is immediately evident that for the first millimeter of the single phase simulation nothing of significance occurs. This is the portion in the simulation where the specimen is flattened, similar to clamping in the actual experiment and in the two phase simulation. It is also evident from the figure that there is no clear distinction of when the elongation of the sample initiates. It cannot be assumed to have started the moment a reaction force is recorded, which is approximately between 0.5 mm and 1 mm. It is not unlikely that a reaction force will be observed during the flattening of the specimen due to the uncrimping of fibers. Freed and Doehring [21] stated that a low reaction force is produced by relaxed collagen fibers, which forms a three dimensional helical structure, when unfolded by stretching. The process of stretching the relaxed fibers is also known as uncrimping. Once the fibers are straightened they become very stiff, which gives rise to the immediate non-linear behaviour observed in Fig. 6.

The question now arises, how does one account for the uncrimping (or flattening) portion obtained from the output during the single phase simulation? There are three methods to account for this portion of the reaction force response: (i) amend the material model with some crimping factor as was done by Studer et al. [15], (ii) compare the numerical results with experimental data to estimate where elongation starts or (iii) simulate the experimental conditions correctly from the start.

Of the three proposed methods to account for the uncrimping of the specimen, the first seems to be the most unlikely approach, unless the study is focussed on developing a constitutive model.

The second approach is to compare the numerical results with experimental data. This approach is illustrated in Fig. 7, where the single phase simulation results are compared to those of the two phase simulation. The two phase simulation is used for comparison as it represents the experimental setup and the material coefficients were optimized using experimental data. It is seen from Fig. 7 that it is required to shift the reaction force results by approximately 2.45 mm and 2.48 mm to the left for Age Group 1 and Age Group 2, respectively. When considering reaction forces greater than 1N, there is good agreement between the single and two phase methods. Even with the shift in the response it is seen that at a displacement of zero, an initial reaction force is observed. This is due to the uncrimping of the fibers in the specimen. When comparing this final result to the experimental data in Fig. 5 it is seen that the experimental data indicates no initial reaction force at a zero displacement. It would appear from these observations that the second approach to account for the uncrimping is also not a desirable approach.

This leaves only the last approach which is to simulate the experimental conditions correctly from the start. The results presented in this study have already indicated that this approach is more desirable than either of the previous two. In Fig. 5 it is clear that by using the two phase method proposed in this study, that the reaction force response is immediately captured as was indicated by experimental data. This approach not only represents the experimental data more accurately, but also requires no additional post processing or time consuming modifications to constitutive models.

CONCLUSION

The objective of this study was to develop a finite element model which is able to accurately represent the strip extensometry experimental setup. Two methods for simulating the strip extensometry test were considered, a single phase and two phase method.

In the single phase method a tension force was applied to the corneal strip, resulting in flattening and elongation of the strip in a single motion. The results indicated that it is difficult to distinguish between the two processes when analysing the reaction force response. This is due to the uncrimping of the fibers in the corneal strip during the flattening process where a low reaction force is observed. This observed reaction force yields doubts as to where exactly the flattening process ends and the elongation process starts. It is believed that there are three methods to account for the flattening process (i) amending the material model with a crimping factor; (ii) comparing the numerical results with the experimental data;

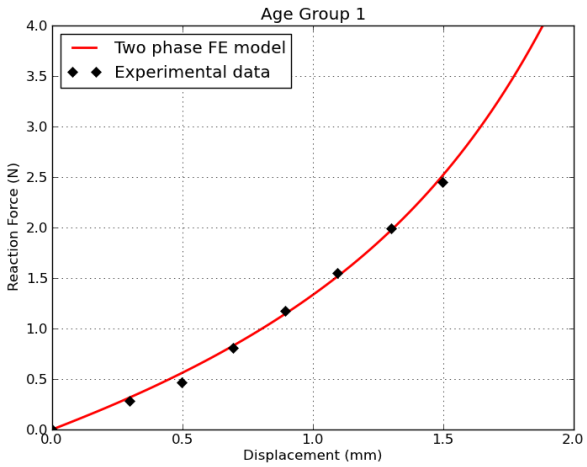

(a) Age Group 1

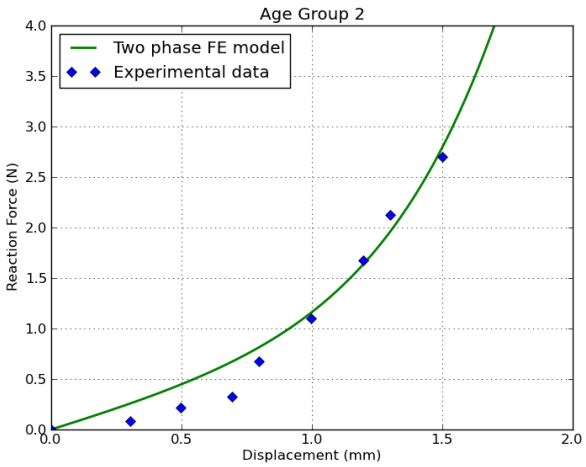

(b) Age Group 2

Fig. 5: Vertical strip extensometry simulation optimization results for Age Group 1 and Age Group 2. Experimental data obtained from Elsheikh et al. [12] is denoted by the black and blue diamonds, and the numerical results obtained in this study by the red and green solid lines.

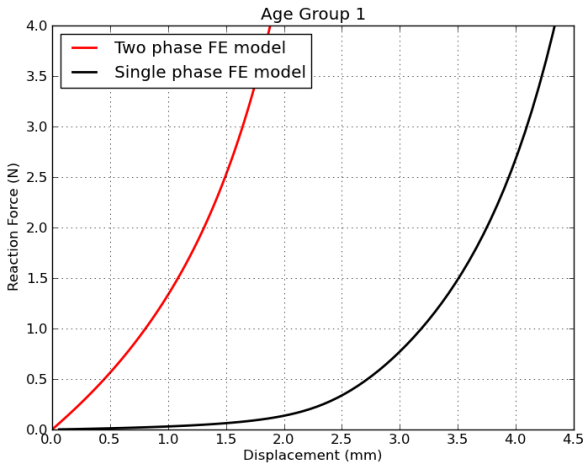

(a) Age Group 1

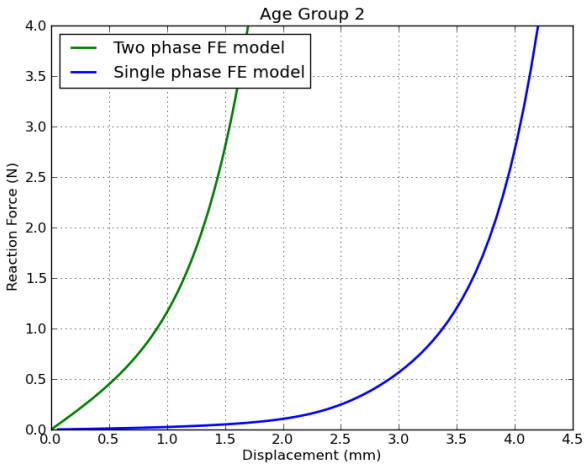

(b) Age Group 2

Fig. 6: Comparison of the vertical strip extensometry simulation results for the single and two phase models for Age Group 1 and Age Group 2. The single phase method is represented by the black and blue curves and the two phase method by the red and green curves.

and (iii) simulating the experimental conditions correctly from the start.

Most researchers will agree that to amend a material model adds an unneccessary complexity to the research and could be time consuming, especially if it is not the focus of a study. For this reason it will be an undesirable method to account for the uncrimping.

The results indicated that by using method (ii) the numerical results still do not accurately represent the experimental data due to the observed reaction forces during uncrimping. The experimental data clearly shows that at zero displacement there is no reaction forces. This discrepancy is indicative of the unreliability of using this method to account for the uncrimping.

This leaves only method (iii) where the experimental conditions are simulated correctly from the start. Using the two phase method the clamping of the corneal specimen is simulated in phase one and the elongation of the strip in the second phase. The results in this study indicated that this method is the more desirable than either of the other two methods considered. No post processing or material model amendments are required to account for uncrimping. Also the reaction force response obtained from the simulation corresponds well with the experimental data.

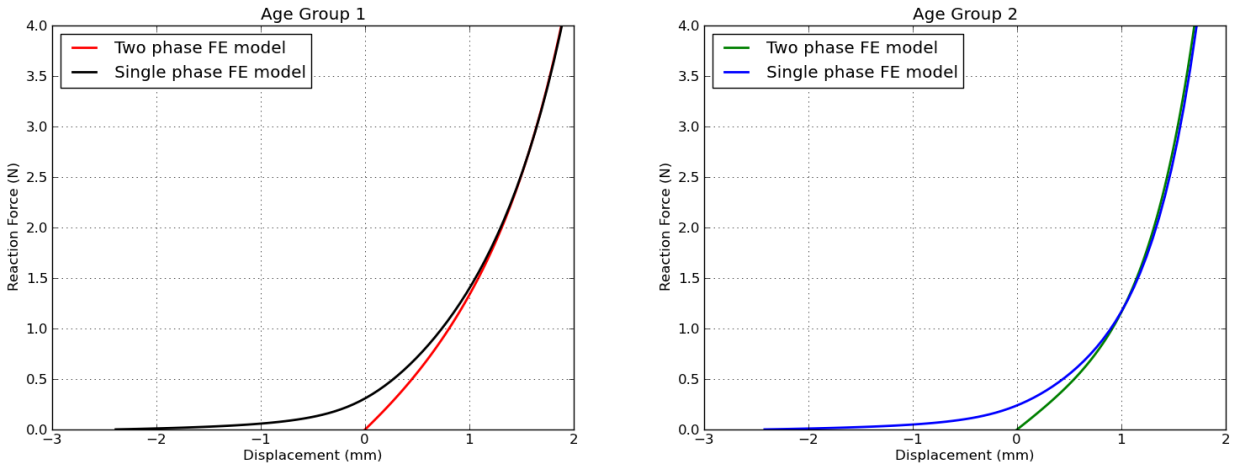

(a) Age Group 1

(b) Age Group 2

Fig. 7: The single phase simulation results are amended and compared with the two phase simulation to determine how much of the curve is due to uncrimping. The single phase method is represented by the black and blue curves and the two phase method by the red and green curves.

This study showed that by accurately simulating the experimental conditions with a well defined finite element model, that no additional work is required to obtain results comparable with experimental data.

Future work will focus on modelling of the diagonal strip extensometry test.

REFERENCES

[1] J. Liu and C. J. Roberts, "Influence of corneal biomechanical properties on intraocular pressure measurement: Quantitative analysis," *Journal of Cataract & Refractive Surgery*, vol. 31, no. 1, pp. 146–155, Jan. 2005. [Online]. Available: http://www.sciencedirect.com/science/article/pii/S0886335004009599

[2] T. Kwon, J. Ghaboussi, D. Pecknold, and Y. Hashash, "Effect of cornea material stiffness on measured intraocular pressure," *Journal of Biomechanics*, vol. 41, no. 8, pp. 1707–1713, 2008. [Online]. Available: http://www.sciencedirect.com/science/article/pii/S002192900800119X

[3] M. R. Bryant and P. J. McDonnell, "Constitutive laws for biomechanical modeling of refractive surgery," *Journal of Biomechanical Engineering*, vol. 118, no. 4, pp. 473–481, Nov. 1996. [Online]. Available: http://link.aip.org/link/?JBY/118/473/1

[4] A. Pandolfi and G. A. Holzapfel, "Three-dimensional modeling and computational analysis of the human cornea considering distributed collagen fibril orientations," *Journal of Biomechanical Engineering*, vol. 130, no. 6, pp. 061 006–12, Dec. 2008. [Online]. Available: http://link.aip.org/link/?JBY/130/061006/1

[5] A. Elsheikh and D. Wang, "Numerical modelling of corneal biomechanical behaviour," *Computer Methods in Biomechanics and Biomedical Engineering*, vol. 10, no. 2, pp. 85–95, Apr. 2007. [Online]. Available: http://www.tandfonline.com/doi/abs/10.1080/10255840600976013

[6] K. Anderson, A. El-Sheikh, and T. Newson, "Application of structural analysis to the mechanical behaviour of the cornea," *Journal of The Royal Society Interface*, vol. 1, no. 1, pp. 3 –15, Nov. 2004. [Online]. Available: http://rsif.royalsocietypublishing.org/content/1/1/3.abstract

[7] A. Elsheikh and K. Anderson, "Comparative study of corneal strip extensometry and inflation tests," *Journal of The Royal Society Interface*, vol. 2, no. 3, pp. 177 –185, Jun. 2005. [Online]. Available: http://rsif.royalsocietypublishing.org/content/2/3/177.abstract

[8] G. Wollensak, E. Spoerl, and T. Seiler, "Stress-strain measurements of human and porcine corneas after riboflavinultraviolet-a-induced cross-linking," *Journal of Cataract & Refractive Surgery*, vol. 29, no. 9, pp. 1780–1785, Sep. 2003. [Online]. Available: http://www.sciencedirect.com/science/article/pii/S0886335003004073

[9] D. A. Hoeltzel, P. Altman, K. Buzard, and K.-i. Choe, "Strip extensiometry for comparison of the mechanical response of bovine, rabbit, and human corneas," *Journal of Biomechanical Engineering*, vol. 114, no. 2, pp. 202–215, May 1992. [Online]. Available: http://link.aip.org/link/?JBY/114/202/1

[10] Y. Zeng, J. Yang, K. Huang, Z. Lee, and X. Lee, "A comparison of biomechanical properties between human and porcine cornea," *Journal of Biomechanics*, vol. 34, no. 4, pp. 533–537, Apr. 2001. [Online]. Available: http://www.sciencedirect.com/science/article/pii/S0021929000002190

[11] M. R. Bryant, K. Szerenyi, H. Schmotzer, and P. J. McDonnell, "Corneal tensile strength in fully healed radial keratotomy wounds." *Investigative Ophthalmology & Visual Science*, vol. 35, no. 7, pp. 3022 –3031, Jun. 1994. [Online]. Available: http://www.iovs.org/content/35/7/3022.abstract

[12] A. Elsheikh, M. Brown, D. Alhasso, P. Rama, M. Campanelli, and D. Garway-Heath, "Experimental assessment of corneal anisotropy," *Journal of refractive surgery (Thorofare, N.J.: 1995)*, vol. 24, no. 2, pp. 178–187, Feb. 2008, PMID: 18297943. [Online]. Available: http://www.ncbi.nlm.nih.gov/pubmed/18297943

[13] A. Elsheikh, D. Wang, M. Brown, P. Rama, M. Campanelli, and D. Pye, "Assessment of corneal biomechanical properties and their variation with age," *Current Eye Research*, vol. 32, no. 1, pp. 11–19, Jan. 2007. [Online]. Available: http://informahealthcare.com/doi/abs/10.1080/02713680601077145

[14] A. Pandolfi and F. Manganiello, "A model for the human cornea: constitutive formulation and numerical analysis," *Biomechanics and Modeling in Mechanobiology*, vol. 5, no. 4, pp. 237–246, Jan. 2006. [Online]. Available: http://www.springerlink.com/content/4vjmr074016g4650/

[15] H. Studer, X. Larrea, H. Riedwyl, and P. Bchler, "Biomechanical model of human cornea based on stromal microstructure," *Journal of Biomechanics*, vol. 43, no. 5, pp. 836–842, Mar. 2010. [Online]. Available: http://www.sciencedirect.com/science/article/pii/S0021929009006678

[16] J. W. Ruberti, A. Sinha Roy, and C. J. Roberts, "Corneal biomechanics and biomaterials," *Annual Review of Biomedical Engineering*, vol. 13, pp. 269–295, Aug. 2011, PMID: 21568714. [Online]. Available: http://www.ncbi.nlm.nih.gov/pubmed/21568714

[17] G. D. C. Dhondt, "Calculix: A free software three-dimensional structural finite element program," 1998.

[18] G. A. Holzapfel, T. C. Gasser, and R. A. Y. W. Ogden, "A new constitutive framework for arterial wall mechanics and a comparative

study of material models," *Journal of Elasticity*, vol. 61, no. 1, pp. 1–48, 2000.

[19] L. G. Carney, J. C. Mainstone, and B. A. Henderson, "Corneal topography and myopia. a cross-sectional study." *Investigative Ophthalmology & Visual Science*, vol. 38, no. 2, pp. 311 –320, Feb. 1997. [Online]. Available: http://www.iovs.org/content/38/2/311.abstract

[20] Scipy Community, "Scipy," Mar. 2011. [Online]. Available: http://docs.scipy.org/doc/

[21] A. D. Freed and T. C. Doehring, "Elastic model for crimped collagen fibrils," *Journal of Biomechanical Engineering*, vol. 127, no. 4, p. 587, 2005. [Online]. Available: http://link.aip.org/link/JBENDY/v127/i4/p587/s1Agg=doi

[22] Python Software Foundation, "Python," Oct. 2011. [Online]. Available: http://www.python.org/doc/

[23] Kitware, Inc., "Paraview," Mar. 2011.